Real-time optimization of the key filtration parameters in an AnMBR: Urban wastewater mono-digestion vs. co-digestion with domestic food waste

A Robles, Gabriel Capson-Tojo, M V Ruano, A Seco, J Ferrer

Elsevier Editorial System(tm) for Waste Management

Manuscript Draft

Manuscript Number: WM-18-597

Title: Real-time optimization of the key filtration parameters in an AnMBR: urban wastewater mono-digestion vs. co-digestion with domestic food waste

Article Type: Full Length Article

Keywords: Anaerobic membrane bioreactor (AnMBR); process control; kitchen waste; fouling; modelling; urban wastewater

Corresponding Author: Dr. Ángel Robles, Ph.D.

Corresponding Author's Institution: Universitat de València

First Author: Ángel Robles, Ph.D.

Order of Authors: Ángel Robles, Ph.D.; Gabriel Capson-Tojo; María Victoria Ruano; Aurora Seco; José Ferrer

Abstract: This study describes a model-based method for real-time optimization of the key filtration parameters in a submerged anaerobic membrane bioreactor (AnMBR) treating urban wastewater (UWW) and UWW mixed with domestic food waste (FW). The method consists of three statistical analyses: (1) Morris screening method to identify the key filtration parameters; (2) Monte Carlo method to establish suitable initial control inputs values; and (3) optimization algorithm for minimizing the operating costs. The operating filtration cost after implementing the control methodology was €0.047 per m3 (59.6% corresponding to energy costs) when treating UWW and €0.067 per m3 when adding FW due to higher fouling rates. However, FW increased the biogas productivities, reducing the total costs to €0.035 per m3. Average downtimes for reversible fouling removal of 0.4% and 1.6% were obtained, respectively. The results confirm the capability of the proposed control system for optimizing the AnMBR performance when treating both substrates.

Suggested Reviewers: Ilse Smets
Professor, Faculty of Engineering Science, KU Leuven
ilse.smets@kuleuven.be
Expertise on Anaerobic Membrane Bioreactors

Adam Smith
Professor, Astani Department of Civil and Environmental Engineering, University of Southern California
smithada@usc.edu
Expertise on Anaerobic Membrane Bioreactors for food waste and urban wastewater treatment

Ignasi Rodríguez-Roda i Layret
Professor, ENGINYERIA QUÍMICA, AGRÀRIA I TECNOLOGIA AGROALIMENTÀRIA, University of Girona
irodriguezroda@icra.cat
Expertise on Membrane Bioreactors Control and Modelling

Dear Editor,

Attached you will find the manuscript entitled "**Real-time optimization of the key filtration parameters in an AnMBR: urban wastewater mono-digestion *vs.* co-digestion with domestic food waste**" submitted for publication as an original article in *Waste Management*. All the authors mutually agree for submitting this manuscript to *Waste Management*, within the category *5.003: Biological-anaerobic (anaerobic digestion)*. We confirm that it is an original work and that the information presented is not being considered for publication in any other journal.

This study describes a model-based method for real-time optimization of the key filtration parameters in a submerged anaerobic membrane bioreactor (AnMBR) treating urban wastewater (UWW) and a mixture of UWW and domestic food waste (FW). Hence, the main aim of this study was to design a competitive and feasible control system capable of enhancing filtration in industrial-scale AnMBR systems with minimum operating costs.

The novelty of this study lies in gaining more insight into the optimization of an AnMBR system at industrial scale. Indeed, to obtain representative results that could be extrapolated to full-scale plants, this study was carried out using data from an AnMBR system featuring industrial hollow-fibre (HF) membranes.

The important findings that must be highlighted are:

- The operating filtration cost after implementing the proposed control methodology was about €0.047 per influent m^3 when treating UWW (59.6 % corresponding to energy costs) and €0.067 per m^3 when adding FW due to higher fouling rates.
- FW also increased the biogas productivities, reducing the total costs to €0.035 per m^3.
- Average downtimes for reversible fouling removal of 0.4 % and 1.6 % were obtained when treating UWW and a mixture of UWW and FW, respectively.
- The results confirm the capability of the proposed control system for optimizing the AnMBR performance when treating both UWW and a mixture of UWW and FW.

To the knowledge of the authors, no other study has been carried out for the optimization of the proposed process using the described methodology.

Yours sincerely,

Ángel Robles Martínez, PhD
Departament d'Enginyeria Química, ETSE-UV.
Universitat de València
Avinguda de la Universitat s/n, 46100, Burjassot, València, Spain
Tel.: +34 96 354 30 85
E-mail: angel.robles@uv.es

Highlights

- Average costs of €0.047 (UWW) and €0.067 per m^3 (UWW and FW) were obtained
- Energy costs accounted for 59.6% and 69.0% of the total costs respectively
- Average reversible fouling removal downtimes were 0.4% and 1.6% respectively
- Control strategy efficiently minimized filtration costs for both substrates

Real-time optimization of the key filtration parameters in an AnMBR: urban wastewater mono-digestion *vs.* co-digestion with domestic food waste

A. Robles [a,*], G. Capson-Tojo [b], M. V. Ruano [a], A. Seco [a], J. Ferrer [c]

[a] CALAGUA – Unidad Mixta UV-UPV, Departament d'Enginyeria Química, ETSE-UV, Universitat de València, Avinguda de la Universitat s/n, 46100, Burjassot, València, Spain.

[b] LBE, INRA, Univ. Montpellier, 102 avenue des Etangs, 11100, Narbonne, France

[c] CALAGUA – Unidad Mixta UV-UPV, Institut Universitari d'Investigació d'Enginyeria de l'Aigua i Medi Ambient – IIAMA, Universitat Politècnica de València, Camí de Vera s/n, 46022, València, Spain

[*] Corresponding author: tel. +34 96 354 30 85, e-mail: *angel.robles@uv.es*

Abstract

This study describes a model-based method for real-time optimization of the key filtration parameters in a submerged anaerobic membrane bioreactor (AnMBR) treating urban wastewater (UWW) and UWW mixed with domestic food waste (FW). The method consists of three statistical analyses: (1) Morris screening method to identify the key filtration parameters; (2) Monte Carlo method to establish suitable initial control inputs values; and (3) optimization algorithm for minimizing the operating costs. The operating filtration cost after implementing the control methodology was €0.047 per m^3 (59.6% corresponding to energy costs) when treating UWW and €0.067 per m^3 when adding FW due to higher fouling rates. However, FW increased the biogas productivities, reducing the total costs to €0.035 per m^3. Average downtimes for reversible fouling removal of 0.4% and 1.6% were obtained, respectively. The results confirm the capability of the proposed control system for optimizing

the AnMBR performance when treating both substrates.

Keywords

Anaerobic membrane bioreactor (AnMBR); process control; kitchen waste; fouling; modelling; urban wastewater

1. Introduction

Submerged anaerobic membrane bioreactors (AnMBRs) are amongst the most promising technologies for treatment of urban wastewater (UWW) (Ben and Semmens, 2002). When compared with traditional processes, such as conventional activated sludge system, AnMBRs offer several advantages (Judd and Judd, 2011; Raskin, 2012): (i) uncoupling of hydraulic retention time (HRT) and solids retention time (SRT), (ii) improvement of organic matter removal efficiency, (iii) reduction of the environmental footprint of the treatment process, (iv) production of a solids-free purified effluent, (v) smaller amounts of sludge produced due to the low biomass yield of anaerobic microorganisms, (vi) lower energy demands (no aeration needed), and (vii) energy recovery by biogas production. In addition, the co-digestion in AnMBRs of UWW with domestic food waste (FW) is a very interesting option which may serve to enhance the biogas productivities (*i.e.* by increasing the organic loading rate and the influent COD/SO_4^{2-} ratio), thus improving the general economics of the treatment process (Becker et al., 2017). Moreover, this approach creates an opportunity for recycling energy and nutrients from both wastes (Kibler et al., 2018). This strategy also allows the valorization of domestic FW, whose anaerobic mono-digestion is known to be associated with several complications, such as accumulation of NH_3 and volatile fatty acids (VFAs) (Capson-Tojo et al., 2017, 2016).

However, a key issue exists that affects the economics of membrane filtration processes and

50 therefore its industrial applicability: membrane fouling (Deng et al., 2016; Sheets et al.,
51 2015). Fouling reduces the permeability of the membrane, which leads to an increase in the
52 operating and maintenance costs, jeopardizing the global performance (Judd and Judd, 2011).
53 Moreover, previous studies have suggested that fouling issues tend to get worse if adding FW
54 to the UWW (Pretel et al., 2016). Thus, if AnMBRs are to be a competitive alternative for
55 UWW treatment from an economical point of view, minimizing the impact of membrane
56 fouling is of critical importance. Therefore, one of the main challenges of this technology is to
57 optimize the treatment performance (keeping high treatment flow rates) and the energy
58 consumption (small physical cleaning intensities and periods) whilst minimizing the fouling
59 effect. Particularly, avoiding irreversible fouling, which must be removed chemically and
60 eventually determines the lifespan of the membranes, is of critical importance (Drews et al.,
61 2009; Judd and Judd, 2011). Moreover, as the physical cleaning of the membranes can
62 account for more than 75 % of the energetic consumption in AnMBRs (Verrecht et al., 2010),
63 this step must also be optimized, reducing as much as possible its frequency.
64 In this respect, the development of advanced control systems is crucial for a successful
65 optimization of the process performance in AnMBRs (Jimenez et al., 2015; Nguyen et al.,
66 2015). Different studies have assessed theoretically (and sometimes validated experimentally)
67 the energy and economical savings resulting from the implementation of different types of
68 advanced control systems in aerobic membrane reactors (MBRs) (Drews et al., 2007;
69 Huyskens et al., 2011). Mannina and Cosenza (2013) applied Monte Carlo simulations to
70 compare the energy requirements, the effluent quality and the economic costs of five different
71 scenarios based on an MBR model. Also, an ad-hoc platform constructed over the
72 COST/Benchmark Simulation Model No. 1 (BSM1) (Coop, 2002) was applied to evaluate
73 different control strategies in MBRs, using the energy requirements to assess the
74 performances (Maere et al., 2011). Gabarron et al. (2014) compared different optimization

strategies applied to MBRs, reducing significantly the energy needs and the membrane fouling. Moreover, Ferrero et al. (2011a, 2011b, 2011c) reduced significant the energy requirements due to membrane scouring (up to 21%) by applying a knowledge-based control system based on a supervisory controller. Focusing on model-based control, Drews et al. (2009, 2007) created a control system based on a mathematical model that successfully improved the filtration efficiency. In addition, Busch et al. (2007) developed a run-to-run control system to optimize the filtration performance by adjusting the filtration variables after each filtration cycle. Recently, computational fluid dynamics simulations have also been applied to optimize membrane scouring and the hydrodynamics in airlift external circulation MBRs (Yang et al., 2017, 2016). These studies allowed a significant reduction of reversible fouling due to cake formation, thus maximizing the MBR performance.

However, so far few control strategies have been developed and validated to optimize the performance of AnMBRs for the treatment of UWW (Robles et al., 2013a). In Robles et al. (2013a), an upper layer fuzzy-logic controller efficiently kept low fouling rates, improving the process performance. In addition, a model-based optimization method has also been applied to improve the performance of AnMBRs treating UWW (Robles et al., 2014a). This method was effectively used for optimization of an advanced control system (consisting of an upper-layer fuzzy-logic controller), obtaining energy savings of up to 25 %. Nevertheless, to improve the economic viability of these systems, it is necessary to develop new control strategies that allow the filtration system to work under optimal conditions.

Among the different options that exist, the use of model-based control systems is of interest, not only to control the process performance, but also to predict it, allowing eventually its optimization from an energetic and/or economical approach (Batstone et al., 2015; Gernaey et al., 2004; Martin and Vanrolleghem, 2014). Nonetheless, the predictions based on models are never totally free of uncertainty because models are always a conceptual representation of

reality and are based on assumptions. Moreover, models need to be calibrated, a process that can be arduous. In this context, sensitivity analysis is a powerful tool that can be used for two main purposes: (i) quantifying the effects of the inputs on the outputs of the model and (ii) identifying the most relevant factors and those that can be disregarded, thus simplifying the calibration process (Pianosi et al., 2016).

Therefore, the objective of this study was to develop a model-based control strategy for real-time optimization of the performance of AnMBRs fed with UWW and a mixture of UWW and FW. Specifically, the strategy aimed at optimizing the operating mode of the filtration process in an AnMBR system by dynamic simulations using a previously validated filtration model. The real-time optimization strategy modified the key filtration parameters in the AnMBR according to the operating conditions of the plant, thus minimizing the operating costs in real-time. The applied model was based on an approach previously used for optimizing the input parameters of an advanced control system for filtration in AnMBRs (Robles et al., 2014a). The proposed optimization strategy consists of three sequential statistical methods: (i) a sensitivity analysis to find an identifiable input subset for the filtration process (Morris screening method) (Morris, 1991), (ii) a Monte Carlo procedure to find adequate initial conditions (using the trajectory-based random sampling technique) and (iii) an optimization algorithm to obtain the optimum input combination of values that minimizes the operating costs of the system.

2. Materials and methods

To accomplish the besought goal the first step of the process consisted in a sensitivity analysis that considers the different parameters susceptible to be optimized in a previously chosen model (Robles et al., 2013c, 2013d), thus selecting highly-influential parameters conforming the identifiable input subset to be optimized. Afterwards, the selection of adequate initial

conditions (those leading to local minimal operational costs) of the identifiable input subset was performed via the Monte Carlo method. Knowing these values, the optimization of the highly-influential operational parameters was carried out. With this purpose, an optimization algorithm was defined. This controller stablished, at every control time (CT), the set points for the operational parameters leading to the lowest costs of the filtration process. Finally, the reduction of the total costs of the filtration process after the implementation of the control system was assessed (with and without FW in the substrate).

2.1. Description of the AnMBR plant

The data used in this study to calibrate and validate the filtration model was obtained from an AnMBR that mainly consisted of an anaerobic reactor with a working volume of 0.9 m^3 connected to two membrane tanks. Each membrane tank had a working volume of 0.6 m^3 and included one ultrafiltration hollow-fibre membrane commercial system (PURON®, Koch Membrane Systems, 0.05 µm pore size, 31 m^2 total filtering area and outside-in filtration). The plant was fully automated and monitored online in real-time. In addition, the anaerobic sludge was sampled once a day to assess the filtration performance. The concentration of mixed liquor total solids (MLTS) was determined according to the Standard Methods (APHA, 2005). A more precise description of the plant and its instrumentation (as well as the corresponding flow diagrams) can be found elsewhere (Robles et al., 2015, 2013b).

2.1.2. Lower-layer controllers

The lower-layer controllers implemented in the system that interact with the proposed optimization method are: (i) three PID controllers that adjust the rotating speed of the sludge recycling pump, the permeate pump and the biogas recycling blower used for membrane scouring by gas sparging; and (ii) one on–off controller that regulates the membrane operating stage by changing the position of the respective on–off valves and the flux direction of the permeate pump. A more precise description of the plant control system can be found

150 elsewhere (Robles et al., 2015).

151 *2.2. Characteristics of the substrates*

152 As aforementioned, the proposed model-based optimisation strategy was validated for an
153 AnMBR treating UWW and a mixture of UWW and FW. To this aim, a filtration model was
154 calibrated and validated using data from an AnMBR system that treated UWW and a mixture
155 of UWW and FW. The UWW was the effluent from the pre-treatment step of the Carraixet
156 WWTP (Valencia, Spain) and the FW was collected from canteens in the university (Moñino
157 et al., 2016). The FW was grinded by an experimental set-up simulating a household grinding
158 system. This set-up consisted on a grinded InSinkErator, model Evolution 100. Afterwards,
159 the FW was pre-filtered using a mesh of 0.5 mm, similar to the one used for the UWW.
160 Further details can be found elsewhere (Moñino et al., 2017).

161 *2.3. Description of the filtration model*

162 The filtration model used in this study is a semi-empirical model based on a classical
163 resistance-in-series model (Robles et al., 2013c). This model is able to represent the dynamic
164 evolution of the transmembrane pressure (TMP) by equations 1 and 2.

$$TMP(t) = J_{net} \cdot \mu_p \cdot R_T \qquad \text{(Eq. 1)}$$

165 Where, TMP (t) is the TMP at time t, μ_p is the dynamic viscosity of the permeate and R_T is
166 the total filtration resistance.

$$R_T = R_M + R_C + R_I = R_M + \omega_C \cdot \alpha_C + \omega_I \cdot \alpha_I \qquad \text{(Eq. 2)}$$

167 Where, R_M is the resistance intrinsic to the membrane, R_C is the resistance of the cake that is
168 formed on the surface of the membrane due to solid deposition, R_I is the added resistance due
169 to irreversible membrane fouling, ω_C is the mass of solids deposited on the membrane per
170 membrane area, α_C is the average specific resistance of the cake created, ω_I is the mass of
171 irreversible fouling normalized per membrane area and α_I is the average specific resistance of

172 the irreversible fouling.

173 The dynamics of ω_C and ω_I were modelled using a black-box approach. With this purpose,
174 three different components were defined: X_{TS} (MLTS), X_{mC} (cake dry mass in the membrane
175 surface), and X_{mI} (irreversible fouling dry mass on the membrane surface). In addition, four
176 kinetic physical processes were included in the model: (i) cake layer formation during
177 filtration, (ii) cake layer removal by biogas sparging for membrane scouring, (iii) cake layer
178 removal by back-flushing and (iv) irreversible fouling formation. A more precise description
179 of the structure of the filtration model can be found elsewhere (Robles et al., 2014a).

180 The selected filtration model was calibrated and validated using experimental data from the
181 above-introduced AnMBR plant when treating UWW and a mixture of UWW and FW.

182 *2.4. Model-based optimization*

183 As aforementioned, the first stage of the optimization process is the selection of the
184 operational parameters associated with the filtration process that are susceptible to be
185 optimized dynamically. These variables are the biogas recycling flow-rate for membrane
186 cleaning (BRF), the sludge recycling flow-rate into the membrane tanks (SRF), the duration
187 of the filtration, relaxation and back-flushing stages (t_F, t_R and t_{BF} respectively) and the
188 initiation frequency and transmembrane flow of the back-flushing stage (f_{BF}, J_{BF}). It must be
189 commented that the transmembrane flow during filtration (J_F) has not been considered for the
190 optimization. The reason is that this value will be fixed by the influent flow-rate to the
191 system.

192 Considering these selected variables, the operating mode of the membranes can be
193 represented by Figure 1A. As this figure shows, an alternation is established between the
194 relaxation and the back-flushing stages. More precisely, if the number of filtration cycles (f) is
195 lower than f_{BF}, the system will alternate between filtration and relaxation cycles. However, if
196 f_{BF} is equal or overpasses f, the corresponding relaxation stage will be substituted by a back-

197 flushing stage. Figure 1B shows a schematic representation of the optimization methodology
198 applied in this study, which is based on a previously proposed real-time optimization
199 procedure and uses the previously introduced filtration model for calculations (Robles et al.,
200 2014a). First of all, the Morris screening method (Morris, 1991) was used to perform a global
201 sensitivity analysis (GSA) of the selected filtration model (step a) to identify the operational
202 parameters with high influence on the cost of the filtration process (step b). Once these
203 parameters were identified, the Monte Carlo procedure (see for instance Saltelli et al. (2000)
204 was applied to determine the optimal initial values of the evaluated parameters (step c). These
205 values are used to update the initial set-points of the operational parameters (step d), which
206 are transferred to the process (step e). After the transmission of the initial set-points, every CT
207 the optimization algorithm is started. In this work CT has been set to 1 hour. This supervisory
208 controller calculates the new optimal set-points for the highly-influential operational
209 parameters at each CT (step f) and transmits them (step g) to update again the set-points of the
210 process (steps d and e). To this aim, a cost objective function was used.

211 *2.4.1. Description of the costs objective function*

212 To determine the costs related to energy consumption, the energy requirement of each process
213 was calculated and multiplied by the cost of energy (E_{COST}; € per kWh). In this study E_{COST}
214 was set to €0.138 per kWh, which corresponded to average electricity prices in Spain.
215 The energy requirements of the blower (W_{BRF}) (adiabatic compression), sludge recycling
216 pump (W_{SRF}) and permeate pump for filtration ($W_{filtration}$) or back-flushing ($W_{back\text{-}flusing}$) were
217 calculated as shown in Robles et al. (2014a).
218 The total energetic costs were lumped in a single variable (C_W), which was calculated as the
219 sum of C_{BRF}, C_{SRF} and C_{STAGE}, as shown in Equation 3:

$$C_W = C_{BRF} + C_{SRF} + C_{STAGE} = W_{BRF} \cdot E_{COST} + W_{SRF} \cdot E_{COST} + W_{STAGE} \cdot E_{COST} \quad \text{(Eq. 3)}$$

220 Where, C_W is the total energetic cost, C_{BRF} is the operating cost of membrane scouring by
221 biogas sparging, C_{SRF} is the operating cost of pumping the sludge, C_{STAGE} is the operating cost
222 of pumping permeate during the respective operating stage (*i.e.* filtration or back-flushing),
223 Finally, in order to determine the combination of operational set-points that lead to the
224 minimal value of the total operating costs ($C_{TOTAL;}$ € per m^3), Equation 4 was applied.

$$C_{TOTAL} = C_W + C_{REAGENTS} + C_{LIFESPAN} \quad \text{(Eq. 4)}$$

225 Where, C_W is the total energetic cost, $C_{REAGENTS}$ is the proportional cost of reagents needed to
226 clean the irreversible fouling produced during filtration and $C_{LIFESPAN}$ is the cost of membrane
227 replacement due to irreversible fouling. $C_{REAGENTS}$ and $C_{LIFESPAN}$ were calculated as shown in
228 Robles et al. (2014a).

229 *2.4.2. Global sensitivity analysis: Morris screening method*

230 In this study the Morris screening method (Morris, 1991) has been applied to perform the
231 GSA. This method is a one-factor-at-a-time process based on the generation of representative
232 matrices of the combinations of values of the parameters to evaluate through a random
233 sampling. From the matrices it determines the distribution of elemental effects (EE_i) of each
234 input factor on the model output. Finally, the EE_i distribution (F_i) for each input factor is
235 analyzed to determine the relative importance of the input factors and obtain a good
236 approximation of a GSA.

237 The selected statistical parameters to evaluate these distributions were: the standard deviation
238 (σ) and the absolute mean (μ^*) (see for instance Saltelli et al. (2000) and Campolongo et al.
239 (2007)).

240 In order to elucidate which operational parameters are the most influential on the total
241 filtration cost, the output variable for the GSA in this study was C_{TOTAL} (Eq. 4).

242 A more precise description of the GSA applied in this study can be found elsewhere (Robles

et al., 2014b).

2.4.3. Initial values of the operation parameters: Monte Carlo method

The Monte Carlo method was used for the selection of initial values of the operational parameters close to the minimum (locally) of the function to minimize. This has two main benefits: (i) it improves the results of the dynamical optimization given by the controller and (ii) it gives optimal values of the non-influential parameters, further improving the minimization of C_{TOTAL}. Therefore, the Monte Carlo method was applied as a previous step before the dynamic optimization. The Monte Carlo method consisting on trajectory-based random sampling was used in this study. Hence, the combination of the operational parameters giving the minimum operating cost (Eq. 4) was selected as the initial values of the model-based supervisory controller.

2.4.4. Simulation strategy and model calibration

MATLAB® was used to simulate the filtration process using the previously-introduced model. The Runge-Kutta method (ode45 function in MATLAB®) was used as integration method for solving the differential equations in the model. The model was calibrated using experimental results from operation with both substrates.

2.4.5. Simulations for real-time dynamic optimization of the filtration process

The dynamic optimization of the filtration process was carried out using the costs equation (Eq. 4) as objective function. The optimization algorithm was applied by using the trust region approach (Coleman and Li, 1996), based on the Newton method (LSQNONLIN function in MATLAB®) and the Runge-Kutta method (ode45 function in MATLAB®).

2.4.6. Implementation of the Morris and Monte Carlo methods

In order to obtain results that could be extrapolated to different situations, MLTS concentrations in the entrance of the membrane tanks was ranged from 10 to 20 $g \cdot l^{-1}$ during simulation. In addition, to take into account the typical fluctuations of the flow rate entering a

WWTP, the net transmembrane flow (J_{net}) was also varied. For each concentrations of MLTS, J_{net} was modified from 4 to 12 LMH ($l \cdot h^{-1} \cdot m^{-2}$), following the influent pattern from the model BSM1 (Jeppsson et al., 2006).

The average values of the operational parameters evaluated in this study are shown in Table 1. In addition, the uncertainty considered for the sensitivity analysis (minimum and maximum values) is also presented. The range of values for the set-points of these parameters was established according to a uniform distribution. Finally, the results of the Monte Carlo procedure (which will be discussed afterwards) are also shown in Table 1.

2.4.7. Optimization algorithm

Using UWW as substrate, the performance of the controller (based on the optimization algorithm) was evaluated by simulation using the filtration model described above. The simulation accounted for 24 h of continuous operation and was carried out at four different MLTS concentrations entering the membrane tanks: 11, 13, 15 and 17 $g \cdot l^{-1}$. For the co-digestion experiment (mixture of UWW and FW), the performance of the supervisory controller was also evaluated in an operational period of 24 h with a MLTS concentration of 17 $g \cdot l^{-1}$. This allowed the comparison between both feeding strategies (*i.e.* UWW and mixture of UWW and FW).

During the simulations J_{net} varied according to the dynamic of BSM1 influent (Jeppsson et al., 2006) (see e-supplementary data).

As aforementioned, the CT was set to 1 hour. The computational cost for optimizing dynamically the process was between 1 to 3 minutes (using a PC Intel® CORE™ i5 with 8 GHz of RAM).

3. Results and discussion

3.1. Calibration of the model

Before the application of the model, it was previously calibrated and validated using data

obtained in the AnMBR plant under a wide range of operational conditions. More precisely, the model was validated for different concentrations of MLTS entering the membrane tanks (10-30 $g \cdot l^{-1}$), different J_{net} (4-6 LMH) and different specific demands of gas per square meter of membrane (SDG_m) (0.1-0.5 $m^3 \cdot h^{-1} \cdot m^{-2}$, equivalent to BRFs of 3-15 $m^3 \cdot h^{-1}$). The model was able to predict precisely the behavior of the membrane during the studied operational conditions (R of 0.989). A more precise description of the calibration and validation of the model applied can be found elsewhere (Moñino et al., 2017).

3.2. Sensitivity analysis

3.2.1. Treating urban wastewater

The rankings for the operational parameters according to the sensitivity measurements obtained (μ^* and σ) are presented in Table 2. Only the results for the optimized number of evaluated trajectories (r_{opt}) are shown.

Hierarchical clustering analysis (HCA; R software version 3.2.5.) of the μ^* presented in Table 2 and the ones obtained during r_{opt} determination resulted in three differentiated clusters formed according to the influence of the studied parameters on the model output (see e-supplementary data): (i) BRF, with a much higher value of μ^* when compared with the other parameters, indicating its great importance for the process costs; (ii) f_{BF}, t_{BF}, t_F and SRF, with values of μ^* that indicate a significant relative influence on the process costs; and (iii) t_R and J_{BF}, with a low relative importance. According to these results, 5 parameters were identified as highly influential on the process costs: (i) BRF ($\mu^* = 1.253$ and $\sigma = 1.856$); (ii) f_{BF} ($\mu^* = 0.770$ and $\sigma = 2.220$); (iii) t_F ($\mu^* = 0.724$ and $\sigma = 1.921$); (iv) t_{BF} ($\mu^* = 0.574$ and $\sigma = 1.210$); and (v) SRF ($\mu^* = 0.464$ and $\sigma = 1.584$). To allow a visual identification of these parameters, a graphical representation of the results of the sensitivity parameters (μ^* and σ) at r_{opt} can be found in the Electronic Annex. Both the clustering and the graphical results suggest a high influence of BRF, SRF, t_F, t_{BF} and f_{BF} on the cost of the process. Therefore, in this study they

have been optimized dynamically as a function of the operational conditions. On the other hand, as t_R and J_{BF} present low values of μ^* and σ, it can be considered that their influence on the total costs is low. Thus, their set-points were considered to be constant, keeping the initial values given by the Monte Carlo method. In addition, the GSA results allow evaluating the mathematical relationship between each parameter and the total costs. Due to their relative high values of both μ^* and σ, the effects of BRF, SRF, t_F, t_{BF} and f_{BF} can be classified as non-linear.

The huge influence of BRF was related to the high energy consumption of this process. Thus, while an adequate value of BRF allows minimizing the solid cake formation, the irreversible fouling rates and the costs associated with biogas recirculation, too high values increase greatly the total costs of the filtration process. Concerning SRF, this parameter affects, not only the costs associated with sludge pumping, but also $MLTS_{MT}$ at a given J_{net}. It is important to consider that changes of the $MLTS_{MT}$ modify also the BRF requirements. In addition, t_F affects the amount of solids that are deposited onto the surface of the membranes. t_F also influences the net water treatment flow, thus determining the normalized profitability of the process (expressed in € per m^3). Finally, t_{BF} and f_{BF} modify the extent of permeability recovery of the membranes. This is related to a partial or total removal of the solid cake. However, it must also be considered that high values of t_{BF} and f_{BF} decrease J_{net} and increase the non-filtration period of the AnMBR.

3.2.2. Treating urban wastewater and food waste

The values of the sensitivity measurements (μ^* and σ) obtained for the optimized number of evaluated trajectories (r_{opt} = 40) when using UWW and FW as substrates are presented in Table 2. The corresponding HCA (see e-supplementary data) resulted in very similar clusters when compared to the process treating only UWW. In this case, 5 main clusters were obtained: (i) BRF, again with a much higher value of μ^* when compared with the other

parameters; (ii) f_{BF}, with higher relative values when compared to treatment of only UWW; (iii) t_{BF} and t_F, also with values of μ^* that indicate a significant relative influence; (iv) SRF and t_R, with a low relative influence; and (v) J_{BF}, with a very low relative importance. The similar responses of the systems fed with UWW and the mixture of UWW and FW confirm the applicability of the optimization methodology evaluated in this study to both substrates. In order to allow an un-biased comparison of the performances of the supervisory controller using both substrates, the same five operational parameters were identified as influential: BRF, f_{BF}, t_{BF}, t_F and SRF. However, it must be considered that the clustering results suggest that in this case SRF could also be kept constant, reducing even more the computational costs. As for the case using UWW as substrate, a graphical representation of the obtained sensitivity rankings treating the UWW and FW mixture is presented in the Electronic Annex.

3.3. Initial parameter estimation via the Monte Carlo method

As aforementioned, the Monte Carlo method was used to estimate the initial values of the different operational parameters object of study when applying both feeding strategies (*i.e.* UWW and mixture of UWW and FW). The total filtration cost varied greatly, with values ranging between €0.04 per m^3 and €0.40 per m^3. Therefore, it can be concluded that the total costs can be effectively minimized by selecting the proper set-points of the selected operational parameters.

The obtained results, which correspond to the combination leading to minimum local costs, are presented in Table 1 (column Monte Carlo Results). However, it is important to highlight that the Monte Carlo method cannot give an optimal combination of the operational parameters. This occurs because of the discrete variation of the values of the evaluated parameters chosen to carry out the simulations. Nevertheless, as the used sampling procedure aims at covering all the domain of variation of the parameters, the cost is locally minimized. Starting from the initial combination given by the Monte Carlo method, the selected

parameters were optimized dynamically throughout the operational period.

3.4. Performance of the supervisory controller

3.4.1. Treating urban wastewater

Figure 2 shows the values of BRF, SRF, t_F and t_{BF} optimized by the controller during the simulations performed with a MLTS concentration entering the membrane tank of 17 $g \cdot l^{-1}$ and the transmembrane fluxes shown in the e-supplementary data. This condition is presented because of two main reasons: (i) it allows comparing the performance of the controller using both substrates and (ii) it is the worst case scenario, meaning that in reality the performance should be improved, with less fouling and lower filtration costs when reducing $MLTS_{MT}$.

As shown in Figure 2A, the value of BRF followed a very similar pattern when compared to J_{net}. This occurred because the controller established higher values of BRF in the periods when the treatment flow rate was the highest (10-13 hours). During those flow peaks, the velocity of solid deposition on the surface of the membrane was much higher than at regular operation and therefore the controller had to increase considerably BRF to keep the TMP at appropriate values. In addition, Figure 2A also shows that the value of BRF was reduced when the treatment flow decreased, reaching even the minimum BRF value allowed in the AnMBR plant (4 $m^3 \cdot h^{-1}$). These conditions corresponded to the minimal membrane fouling propensity, but were also associated with low agitation of the sludge in the membrane tanks, leading to a reduction in the efficiency of the process of physical cleaning by biogas sparging.

A correlation matrix including the optimized parameters, $MLTS_{MT}$, J_{net}, TMP, the energy requirements and the filtration costs with UWW as substrate (see e-supplementary data; R software version 3.2.5.) verified the positive correlation observed between J_{net}, TMP and BRF.

Regarding SRF, Figure 2A shows a similar behavior to that observed for BRF. The controller increased SRF at higher J_{net} to keep $MLTS_{MT}$ at adequate levels. Again, the correlation matrix

verified the correlation existing between BRF and SRF.

Concerning t_F and t_{BF}, it can be observed in Figure 2B that in this case these variables did not follow a pattern similar to that of J_{net}. However, a variation of these parameters occurred through the operational period studied. Interestingly, the periods when t_F and t_{BF} varied the most were those when BRF and SRF showed their lowest values (*i.e.* 5-9 h and 19-24 h). This indicates that, when the controller could not further optimize BRF and SRF, it modified the parameters with lower influence (*i.e.* t_F and t_{BF}) to further minimize the total filtration costs. No linear correlations were observed between t_F and t_{BF} and any other studied parameter/variable (see e-supplementary data). The last parameter to be discussed (f_{BF}) remained relatively constant, around 1 BF every 10 F cycles (see Figure 3).

Figure 3 represents the evolution of the TMP and the sequence of operational stages (F, R and BF) performed during the simulation at 17 $g \cdot l^{-1}$ MLTS entering the membrane tanks.

As it can be observed, the operational mode varied according to the duration of the stages (t_F and t_{BF}). In addition, by increasing SRF and BRF (Figure 2A) during the periods most prone to fouling (hours 10-12), the supervisory controller was able to keep the TMP under the maximum limits established by the provider (*i.e*. 0.6 bars).

3.4.2. Treating urban wastewater and food waste

Figure 4 shows the values of BRF, SRF, t_F and t_{BF} optimized by the supervisory controller when treated UWW and FW. As for the operation with UWW as substrate (Figure 2A), the values of BRF and SRF varied according to the variations in J_{net} (see e-supplementary data). As previously, the controller established higher values of both parameters at the points of highest J_{net} (10-13 hours). This period corresponded to the greatest rates of solids deposition onto the membranes. Therefore, the controller increased BRF to reduce the fouling rate and increased also SRF to minimize $MLTS_{MT}$.

In addition, it can be observed in Figure 4B that the values of t_F are lower than those obtained

418 with UWW as substrate (Figure 2B). Interestingly, the opposite occurred for t_{BF}, whose length
419 was higher with the mixture of UWW and FW. This was related to a more intense fouling
420 caused by the FW, which led to longer BF periods to remove the cake layer from the
421 membrane surface. Moreover, f_{BF} increased from 1 BF every 10 F cycles to 1 BF every 4 F
422 cycles (data not shown). Longer t_{BF} and higher f_{BF} with FW led to an increase of the
423 downtime for reversible fouling removal. The average downtime for reversible fouling
424 removal increased from 0.4 % (UWW) to 1.6 % (UWW and FW) of the total operational
425 period. Nevertheless, it must be considered that these are low values which were achieved as a
426 result of the controller action. As example, previous studies have reported minimum values of
427 2.4 % of downtime when treating UWW in an automatically-tuned advanced control system
428 for AnMBRs (Robles et al., 2014a).
429 It must be mentioned that the corresponding correlation matrix (see e-supplementary data)
430 was very similar to that obtained for UWW as substrate, verifying that the controller
431 responded in a similar manner for both substrates. Also, as the evolution of the TMP and the
432 different stages simulated using the substrate mixture were similar to that of UWW treatment
433 (Figure 3), these values are not presented.
434 *3.5. Total energy consumption*
435 Figure 5A shows the evolution of the energy requirements of the filtration process after the
436 implementation of the supervisory controller at 17 $g \cdot l^{-1}$ MLTS entering the membrane tank
437 with UWW as substrate. As it can be observed, the main contributor to the energy
438 consumption of the system was W_{BRF}, accounting in average for 80 % of the total energy
439 requirements and up to 87 % at the highest J_{net}. In addition, W_{BRF} (thus W_{TOTAL}) shows a
440 similar pattern to that observed for J_{net}. In fact, both variables were strongly correlated (see e-
441 supplementary data). While during the periods of low inflow to the plant (*i.e.* hours 2-9)
442 W_{TOTAL} reached 0.13 $kWh \cdot m^{-3}$ (with W_{BRF} accounting for 67 %), this value increased up to

0.34 kWh·m^{-3} (with W_{BRF} accounting for 87 %) at high J_{net} (*i.e.* hours 9-12). At this point it must be mentioned that the results shown in this study were obtained with a model calibrated using considerably dirty membranes (i.e. the membranes were already strongly irreversibly fouled). Therefore, the energy requirements presented correspond to a very unfavorable scenario and it can be expected that their values will be considerably lower when operating with clean membranes. Nevertheless, the proposed control strategy allowed keeping the W_{BRF} within low values (around 0.18 kWh·m^{-3}). More precisely, the supervisory control system led to savings of around 50 % of the energy required for membrane scouring when compared to non-optimized cyclic operation of the same AnMBR plant (0.36 kWh·m^{-3}) (Robles et al., 2013a). By coupling model-based control systems with fuzzy-logic advanced supervisory control, consumptions of 0.15 kWh·m^{-3} (Robles et al., 2013a) and 0.12 kWh·m^{-3} (Robles et al., 2014a) were achieved. The value obtained in this study was slightly higher (0.18 kWh·m^{-3}). However, it must be considered that in this case only a model must be calibrated, which can be continuously optimized by retrofitting. In addition, if the model is properly calibrated this control strategy is more straight-forward and the control action is faster when compared to the previous control strategies, which require more computational capacity.

When paying attention to the average energy requirements of the AnMBR after the implementation of the control system (Table 3), it can be observed that from the total consumption of 0.20 kWh·m^{-3} (operating at 17 g·l^{-1} MLTS entering the membrane tanks), 79.7 % corresponded to W_{BRF}, 16.9 kWh·m^{-3} to W_{SRF}, 9.53 % to $W_{back\text{-}flushing}$ and 4.77 % to $W_{filtration}$.

The results presented in Figure 5 and Table 3 show that the energy required to clean physically the membranes by biogas sparging (W_{BRF}) represents the main consumption of energy in AnMBRs. Thus, there is a clear need to optimize this particular process.

Figure 5B and Table 3 also show the energy consumption of the filtration process treating

468 UWW and FW. In this case, the average total requirement was 0.34 $kWh \cdot m^{-3}$, with a
469 maximum value of 0.58 $kWh \cdot m^{-3}$. The average proportion of W_{BRF} accounted for 88.5 %,
470 indicating the need of optimizing BRF for each specific process.
471 The higher average W_{TOTAL} when adding FW (0.34 *vs.* 0.20 $kWh \cdot m^{-3}$) was related to the
472 aforementioned increase of the fouling rate in the membranes, which implied longer non-
473 filtration periods, thus reducing the net volume of water treated per unit of membrane surface.
474 However, it must be considered that the addition of FW also led to a higher energy recovery
475 due to an increase of the biogas production. With a SRT of 70 days at a temperature of 27 ºC,
476 the volumetric methane production was up to 72 $l_{CH4} \cdot m^{-3}$ using UWW as substrate (Pretel et
477 al., 2016). When adding FW, this value increased up to 147 $l_{CH4} \cdot m^{-3}$ which, assuming a
478 percentage of methane recovery of 80 %, was translated into an increase of the energy
479 recovery of 0.20 $kWh \cdot m^{-3}$. Taking this value into account, the energy requirements of the
480 filtration process are lowered from 0.34 $kWh \cdot m^{-3}$ to 0.14 $kWh \cdot m^{-3}$, even when operating with
481 strongly fouled membranes. Thus, the addition of FW led to a global energy savings of 30 %
482 when compared to the treatment of UWW as sole substrate. Therefore, it can be concluded
483 that, even if FW was added into the UWW, the supervisory control system allowed operating
484 the AnMBR at low energy costs.
485 *3.6. Total costs*
486 Figure 6A shows the evolution of the operational and maintenance costs of the filtration
487 system after the implementation of the supervisory controller treating UWW at 17 $g \cdot l^{-1}$
488 MLTS. As it can be observed, C_W represented the main cost of the process, accounting for an
489 average of 60 % of the total cost. This clearly emphasizes the need to optimize the operational
490 conditions to minimize the energy demand of the system. However, in the period of peak J_{net}
491 (hours 9-10) the ensemble of $C_{REAGENTS}$ and $C_{LIFESPAN}$ represented up to 90 % of the total
492 costs. This was related to a more intense irreversible fouling occurring in this period of high-

493 rate filtration, which caused an increase in the amounts of chemicals required to clean the
494 membranes and lowered the membrane lifespan, raising the associated costs.
495 Regarding the average costs, the results operating at 17 $g \cdot l^{-1}$ MLTS entering the membranes
496 are presented in Table 4. After the implementation of the control system, C_{TOTAL} was €0.047
497 per m^3, with C_W, $C_{REAGENTS}$ and $C_{LIFESPAN}$ representing the 59.6, 17.0 and 23.4 %,
498 respectively.
499 These values corroborate that C_W represents the main filtration costs during regular operation.
500 In addition, as it has been already mentioned, the membranes used in this study were strongly
501 fouled, and therefore lower costs are expected in real operation. Thus, the values of these
502 latter costs should be lower in full-scale plants, further reinforcing the great importance of
503 optimizing the energy requirement in AnMBR plant.
504 Figure 6B and Table 4 present the costs corresponding to the co-digestion system (UWW and
505 FW). As shown, the obtained pattern was very similar to that obtained for treatment of UWW.
506 However, in this case the average filtration cost corresponded to €0.067 per m^3, with C_W
507 accounting for 69 % of this value. The higher value of C_{TOTAL} when adding FW is again
508 related to a higher fouling rate in the co-digestion system, which led to higher costs associated
509 with the mechanical cleaning of the membrane. This is further suggested by the higher C_W
510 values (€0.046 per m^3 with FW *vs.* €0.028 per m^3 with only UWW).
511 However, when taking into account the economical profit related to the higher volumetric
512 methane production when adding FW to the UWW, C_{TOTAL} is reduced to €0.035 per m^3,
513 meaning that FW addition led a relative economic saving of 26 % of the filtration costs (when
514 compared with the AnMBR system treating only UWW).
515

516 **4. Conclusions**

517 The proposed methodology enabled identifying the most influential filtration parameters and

selecting proper initial set points for their optimization. The controller allowed a real-time optimization of these set-points, obtaining an energy demand of 0.20 $kWh \cdot m^{-3}$ (79.7% W_{BRF}) and a cost of €0.047 per m^3 (59.6% C_W) when treating UWW. The addition of FW increased the energy demand and the costs (0.34 $kWh \cdot m^{-3}$ and €0.067 per m^3) due to higher fouling intensity, but also led to the production of more biogas. The obtained results confirm the applicability of the proposed control system for optimizing the AnMBR performance when treating both substrates.

Acknowledgements

This research work was possible thanks to financial support from Generalitat Valenciana (project PROMETEO/2012/029) which is gratefully acknowledged. Besides, support from FCC Aqualia participation in INNPRONTA 2011 IISIS IPT-20111023 project (partially funded by The Centre for Industrial Technological Development (CDTI) and from the Spanish Ministry of Economy and Competitiveness) is gratefully acknowledged.

References

APHA, 2005. Standard Methods for the Examination of Water and Wastewater. American Public Health Association, Washington, DC.

Batstone, D.J., Puyol, D., Flores-Alsina, X., Rodríguez, J., 2015. Mathematical modelling of anaerobic digestion processes: applications and future needs. Rev. Environ. Sci. Bio/Technology 14, 595–613.

Becker, A.M., Yu, K., Stadler, L.B., Smith, A.L., 2017. Co-management of domestic wastewater and food waste: A life cycle comparison of alternative food waste diversion strategies. Bioresour. Technol. 223, 131–140.

Ben, A., Semmens, M., 2002. Membrane bioreactors for wastewater treatment and reuse: a success story. Water Sci. Technol. 47, 1–5.

Busch, J., Cruse, A., Marquardt, W., 2007. Run-to-run control of membrane filtration processes. AIChE J. 53, 2316–2328.

Campolongo, F., Cariboni, J., Saltelli, A., 2007. An effective screening design for sensitivity analysis of large models. Environ. Model. Softw. 22, 1509–1518.

548 Capson-Tojo, G., Rouez, M., Crest, M., Steyer, J.-P., Delgenès, J.-P., Escudié, R., 2016. Food
549 waste valorization via anaerobic processes: a review. Rev. Environ. Sci. Bio/Technology
550 15, 499–547.

551 Capson-Tojo, G., Rouez, M., Crest, M., Trably, E., Steyer, J., Bernet, N., Delgenes, J.,
552 Escudié, R., 2017. Kinetic study of dry anaerobic co-digestion of food waste and
553 cardboard for methane production. Waste Manag. 69, 470–479.

554 Coleman, T.F., Li, Y., 1996. An interior trust region approach for nonlinear minimization
555 subject to bounds. SIAM J. Optim. 6, 418–445.

556 Coop, J.B., 2002. The COST Simulation Benchmark: Description and Simulator Manual.
557 Luxembourg.

558 Deng, L., Guo, W., Ngo, H.H., Zhang, H., Wang, J., Li, J., Xia, S., Wu, Y., 2016. Biofouling
559 and control approaches in membrane bioreactors. Bioresour. Technol. 221, 656–665.

560 Drews, A., Arellano-Garcia, H., Schöneberger, J., Schaller, J., Kraume, M., Wozny, G., 2007.
561 Improving the efficiency of membrane bioreactors by a novel model-based control of
562 membrane filtration, in: 17th European Symposium on Computer Aided Process
563 Engineering – ESCAPE. pp. 345–350.

564 Drews, A., Arellano-Garcia, H., Schöneberger, J., Schaller, J., Wozny, G., Kraume, M., 2009.
565 Model-based recognition of fouling mechanisms in membrane bioreactors. Desalination
566 236, 224–233.

567 Ferrero, G., Monclus, H., Buttiglieri, G., Comas, J., Rodriguez-Roda, I., 2011. Automatic
568 control system for energy optimization in membrane bioreactors. Desalination 268, 276–
569 280.

570 Ferrero, G., Monclus, H., Buttiglieri, G., Gabarron, S., Comas, J., Rodriguez-Roda, I., 2011.
571 Development of an algorithm for air-scour optimization in Membrane Bioreactors, IFAC
572 Proceedings Volumes (IFAC-PapersOnline). IFAC.

573 Ferrero, G., Monclús, H., Sancho, L., Garrido, J.M., Comas, J., Rodríguez-Roda, I., 2011. A
574 knowledge-based control system for air-scour optimisation in membrane bioreactors.
575 Water Sci. Technol. 63, 2025–2031.

576 Gabarron, S., Ferrero, G., Dalmau, M., Comas, J., Rodriguez-Roda, I., 2014. Assessment of
577 energy-saving strategies and operational costs in full-scale membrane bioreactors. J.
578 Environ. Manage. 134, 8–14.

579 Gernaey, K. V, van Loosdrecht, M.C.., Henze, M., Lind, M., Jørgensen, S.B., 2004. Activated
580 sludge wastewater treatment plant modelling and simulation: state of the art. Environ.
581 Model. Softw. 19, 763–783.

582 Huyskens, C., Brauns, E., Van Hoof, E., Diels, L., De Wever, H., 2011. Validation of a
583 supervisory control system for energy savings in membrane bioreactors. Water Res. 45,
584 1443–1453.

585 Jeppsson, U., Rosen, C., Alex, J., Copp, J., Gernaey, K. V., Pons, M.N., Vanrolleghem, P. a.,
586 2006. Towards a benchmark simulation model for plant-wide control strategy
587 performance evaluation of WWTPs. Water Sci. Technol. 53, 287–295.

588 Jimenez, J., Latrille, E., Harmand, J., Robles, A., Ferrer, J., Gaida, D., Wolf, C., Mairet, F.,
589 Bernard, O., Alcaraz-Gonzalez, V., 2015. Instrumentation and control of anaerobic
590 digestion processes: a review and some research challenges. Rev. Environ. Sci.

591 Bio/Technology 14, 615–648.

592 Judd, S., Judd, C., 2011. The MBR Book: Principles and applications of membrane
593 bioreactors for water and wastewater treatment, 2nd ed. Elsevier, London (UK).

594 Kibler, K.M., Reinhart, D., Hawkins, C., Motlagh, A.M., Wright, J., 2018. Food waste and the
595 food-energy-water nexus: A review of food waste management alternatives. Waste
596 Manag., In Press.

597 Maere, T., Verrecht, B., Moerenhout, S., Judd, S., Nopens, I., 2011. BSM-MBR: A
598 benchmark simulation model to compare control and operational strategies for
599 membrane bioreactors. Water Res. 45, 2181–2190.

600 Mannina, G., Cosenza, A., 2013. The fouling phenomenon in membrane bioreactors:
601 Assessment of different strategies for energy saving. J. Memb. Sci. 444, 332–344.

602 Martin, C., Vanrolleghem, P.A., 2014. Analysing, completing, and generating influent data
603 for WWTP modelling: A critical review. Environ. Model. Softw. 60, 188–201.

604 Moñino, P., Aguado, D., Barat, R., Jiménez, E., Giménez, J.B., Seco, A., Ferrer, J., 2017. A
605 new strategy to maximize organic matter valorization in municipalities: Combination of
606 urban wastewater with kitchen food waste and its treatment with AnMBR technology.
607 Waste Manag. 62, 274–289.

608 Moñino, P., Jiménez, E., Barat, R., Aguado, D., Seco, A., Ferrer, J., 2016. Potential use of the
609 organic fraction of municipal solid waste in anaerobic co-digestion with wastewater in
610 submerged anaerobic membrane technology. Waste Manag. 56, 158–165.

611 Morris, M., 1991. Factorial sampling plans for preliminary computational experiments.
612 Technometrics 33, 239–245.

613 Nguyen, D., Gadhamshetty, V., Nitayavardhana, S., Khanal, S.K., 2015. Automatic process
614 control in anaerobic digestion technology: A critical review. Bioresour. Technol. 193,
615 513–522.

616 Pianosi, F., Beven, K., Freer, J., Hall, J.W., Rougier, J., Stephenson, D.B., Wagener, T., 2016.
617 Sensitivity analysis of environmental models: A systematic review with practical
618 workflow. Environ. Model. Softw. 79, 214–232.

619 Pretel, R., Moñino, P., Robles, A., Ruano, M. V., Seco, A., Ferrer, J., 2016. Economic and
620 environmental sustainability of an AnMBR treating urban wastewater and organic
621 fraction of municipal solid waste. J. Environ. Manage. 179, 83–92.

622 Raskin, L., 2012. Anaerobic membrane bioreactors for sustainable wastewater treatment.
623 WERF report U4R08.

624 Robles, A., Duran, F., Ruano, M.V., Ribes, J., Rosado, A., Seco, A., Ferrer, J., 2015.
625 Instrumentation, control, and automation for submerged anaerobic membrane
626 bioreactors. Environ. Technol. 36, 1–12.

627 Robles, A., Ruano, M.V., Ribes, J., Ferrer, J., 2013a. Advanced control system for optimal
628 filtration in submerged anaerobic MBRs (SAnMBRs). J. Memb. Sci. 430, 330–341.

629 Robles, A., Ruano, M. V., Ribes, J., Ferrer, J., 2013b. Factors that affect the permeability of
630 commercial hollow-fibre membranes in a submerged anaerobic MBR (HF-SAnMBR)
631 system. Water Res. 47, 1277–1288.

632 Robles, A., Ruano, M. V., Ribes, J., Seco, A., Ferrer, J., 2013c. A filtration model applied to

633 submerged anaerobic MBRs (SAnMBRs). J. Memb. Sci. 444, 139–147.

634 Robles, A., Ruano, M. V., Ribes, J., Seco, A., Ferrer, J., 2013d. Mathematical modelling of
635 filtration in submerged anaerobic MBRs (SAnMBRs): Long-term validation. J. Memb.
636 Sci. 446, 303–309.

637 Robles, A., Ruano, M. V, Ribes, J., Seco, A., Ferrer, J., 2014a. Model-based automatic tuning
638 of a filtration control system for submerged anaerobic membrane bioreactors (AnMBR).
639 J. Memb. Sci. 465, 14–26.

640 Robles, A., Ruano, M. V., Ribes, J., Seco, A., Ferrer, J., 2014b. Global sensitivity analysis of
641 a filtration model for submerged anaerobic membrane bioreactors (AnMBR). Bioresour.
642 Technol. 158, 365–373.

643 Saltelli, A., Chan, K., Scott, E.M., 2000. Sensitivity Analysis. John Wiley & Sons, New York.

644 Sheets, J.P., Yang, L., Ge, X., Wang, Z., Li, Y., 2015. Beyond land application: Emerging
645 technologies for the treatment and reuse of anaerobically digested agricultural and food
646 waste. Waste Manag. 44, 94–115.

647 Verrecht, B., Maere, T., Nopens, I., Brepols, C., Judd, S., 2010. The cost of a large-scale
648 hollow fibre MBR. Water Res. 44, 5274–5283.

649 Yang, M., Wei, Y., Zheng, X., Wang, F., Yuan, X., Liu, J., Luo, N., Xu, R., Yu, D., Fan, Y.,
650 2016. CFD simulation and optimization of membrane scouring and nitrogen removal for
651 an airlift external circulation membrane bioreactor. Bioresour. Technol. 219, 566–575.

652 Yang, M., Yu, D., Liu, M., Zheng, L., Zheng, X., Wei, Y., Wang, F., Fan, Y., 2017.
653 Optimization of MBR hydrodynamics for cake layer fouling control through CFD
654 simulation and RSM design. Bioresour. Technol. 227, 102–111.

655

Figure captions

Figure 1. (A) Sequence of the different operational stages in the membrane modules during the alternative operating mode and (B) flow diagram of the proposed optimization methodology

Figure 2. (A) Values of BRF and SRF and (B) t_F and t_{BF} optimized by the supervisory controller. The results were obtained using UWW as substrate

Figure 3. Evolution of the TMPs and different stages simulated. The results were obtained using UWW as substrate

Figure 4. (A) Values of BRF and SRF and (B) t_F and t_{BF} optimized by the supervisory controller. The results were obtained using UWW and FW as substrates

Figure 5. Evolution of the energy requirements of the filtration process with the controller operating at 17 $g \cdot l^{-1}$ MLTS entering the membrane tanks. The results for feeding strategies are shown: (A) UWW and (B) mixture of UWW and FW

Figure 6. Evolution of the costs of the filtration process with the controller operating at 17 $g \cdot l^{-1}$ MLTS entering the membrane tanks. The results for feeding strategies are shown: (A) UWW and (B) mixture of UWW and FW

672 **Table captions**

673 **Table 1.** Average values of the operational parameters evaluated in this study. The intervals
674 of uncertainty, as well as the initial values for the model-based supervisory controller (Monte
675 Carlo results) are also presented

676 **Table 2.** Sensitivity rankings for r_{opt} with UWW as substrate (r_{opt} = 60) and the mixture of
677 UWW and FW (r_{opt} = 40)

678 **Table 3.** Average energy requirements of the filtration process with the controller operating at
679 17 $g \cdot l^{-1}$ MLTS entering the membrane tanks

680 **Table 4.** Average costs of the filtration process with the controller operating at 17 $g \cdot l^{-1}$ MLTS
681 entering the membrane tanks

Supplementary material

Figure S1. Net transmembrane flow (J_{net}) applied during the validation of the supervisory controller by simulation. The corresponding values of the MLTS concentrations in the membrane tanks ($MLTS_{MT}$) during the co-digestion experiment at 17 $g \cdot l^{-1}$ are also shown

Figure S2. TMP simulated by the model (TMP_{sim}) vs experimental TMP (TMP_{exp})

Hierarchical clustering analysis based on the absolute means of the selected parameters with UWW as substrate

Figure S3. Hierarchical clustering analysis based on the absolute means of the selected parameters obtained (A) with **(a)** UWW as substrate and (B) with UWW and FW as substrates

Figure S4. Sensitivity measurements (μ^* and σ) obtained (A) with UWW as substrate (r_{opt} of 60) and (B) with the mixture of UWW and FW as substrate (r_{opt} of 40)

Figure S5. Correlation matrix ($\alpha = 0.05$; $n = 999$) of the optimized parameters, the energy requirements and the filtration costs obtained (A) with UWW as substrate and (B) with mixture of UWW and FW as substrate. The $MLTS_{MT}$, J_{net} and TMP are also included

Abbreviation and symbols

AeMBR - Aerobic membrane bioreactor

AnMBR - Submerged anaerobic membrane bioreactor

BRF – Biogas recycling flow-rate

BF – Back-flushing period

$\mathbf{C_B}$ **–** Operating cost of membrane scouring by biogas sparging

$\mathbf{C_{LIFESPAN}}$ – Cost of membrane replacement due to irreversible fouling.

$\mathbf{C_{REAGENTS}}$ – Cost of reagents needed to clean irreversible fouling

$\mathbf{C_{SRF}}$ – Operating cost of pumping the sludge

$\mathbf{C_{STAGE}}$ – Operating cost of pumping permeate

CT – Control time

$\mathbf{C_{TOTAL}}$ **–** Total operating costs

$\mathbf{C_W}$ – Total energetic cost

D – Pipe diameter

$\mathbf{E_{COST}}$ – Cost of energy

$\mathbf{EE_i}$ – Elemental effects of each input factor on the model output

f – Number of filtration periods

fr – Friction factor

F – Filtration period

$\mathbf{f_{BF}}$ **–** Back-flush frequency

$\mathbf{F_i}$ – Scaled elementary effect distribution

g – Acceleration of gravity

GSA – Global sensitivity analysis

HCA – Hierarchical clustering analysis

HRT – Hydraulic retention time

J_{BF} – Transmembrane flow during back-flush

J_{net} – Net transmembrane flow

L – Pipe length

L_{eq} – Equivalent pipe length of accidental pressure drops

M – Molar flow rate of biogas

MBR - Membrane bioreactor

MLTS – Mixed liquor total solids

$MLTS_{MT}$ – MLTS concentration in the membrane tanks

OFMSW - Organic fraction of municipal solid waste

P_1 – Absolute inlet pressure

P_2 – Absolute outlet pressure

q – Volumetric flow rate

R – Relaxation period

R_g – Ideal gas constant

R_C – Resistance of the solid cake formed on the surface of the membrane

R_I – Resistance due to irreversible fouling of the membrane

R_M – Resistance intrinsic to the membrane

r_{opt} – Optimum number of times that the SEE_i should be calculated

R_T – Total filtration resistance

SEE_i – Scaled elementary effect

SDG_m – Specific demand of gas per square meter of membrane

SRF – Sludge recycling flow-rate

SRT – Solids retention time

t_{BF} – Duration of the back-flushing stage

t_F – Duration of the filtration stage

$\mathbf{T_{gas}}$ – Biogas temperature

TMP – Transmembrane pressure

$\mathbf{TMP_{sim}}$ – Simulated transmembrane pressure

$\mathbf{TMP_{exp}}$ – Experimental transmembrane pressure

TS – Total solids

$\mathbf{t_R}$ **–** Duration of the relaxation stage

UWW - Urban wastewater

V – Fluid velocity

$\mathbf{V_T}$ – Net volume of treated wastewater

$\mathbf{W_{back\text{-}flusing}}$ – Energy requirements of the back-flushing pump

$\mathbf{W_{BRF}}$ – Energy requirements of the biogas lower

$\mathbf{W_{filtration}}$ – Energy requirements of the permeate filtration pump

$\mathbf{W_{SRF}}$ – Energy requirements of the sludge recycling pump

$\mathbf{X_{mC}}$ **–** Dry mass of cake in the membrane surface

$\mathbf{X_{mI}}$ **–** Dry mass of irreversible fouling on the membrane surface

$\mathbf{X_{TS}}$ **–** Concentration of total solids in the mixed liquor

$\mathbf{Z_1\text{-}Z_2}$ – difference in height

α – Compression index

$\mathbf{\alpha_C}$ **–** Average specific resistance of the solid cake

$\mathbf{\alpha_I}$ **–** Average specific resistance of the irreversible fouling

σ – Standard deviation

$\mathbf{\rho_{sludge}}$ – sludge density

$\mathbf{\eta_{blower}}$ – Overall mechanical and electrical efficiency of the blower

$\mathbf{\eta_{pump}}$ – Overall mechanical and electrical efficiency of the pump

μ – Mean

$\boldsymbol{\mu^*}$ **–** Absolute mean (μ^*)

$\boldsymbol{\mu_p}$ **–** Dynamic viscosity of the permeate

$\boldsymbol{\omega_C}$ **–** Mass of solids settled per membrane area

$\boldsymbol{\omega_I}$ **–** Mass of irreversible fouling per membrane area

$\boldsymbol{\Delta R_{I,MAX}}$ – Upper threshold of irreversible fouling resistance at which membrane cleaning starts

Graphical abstract

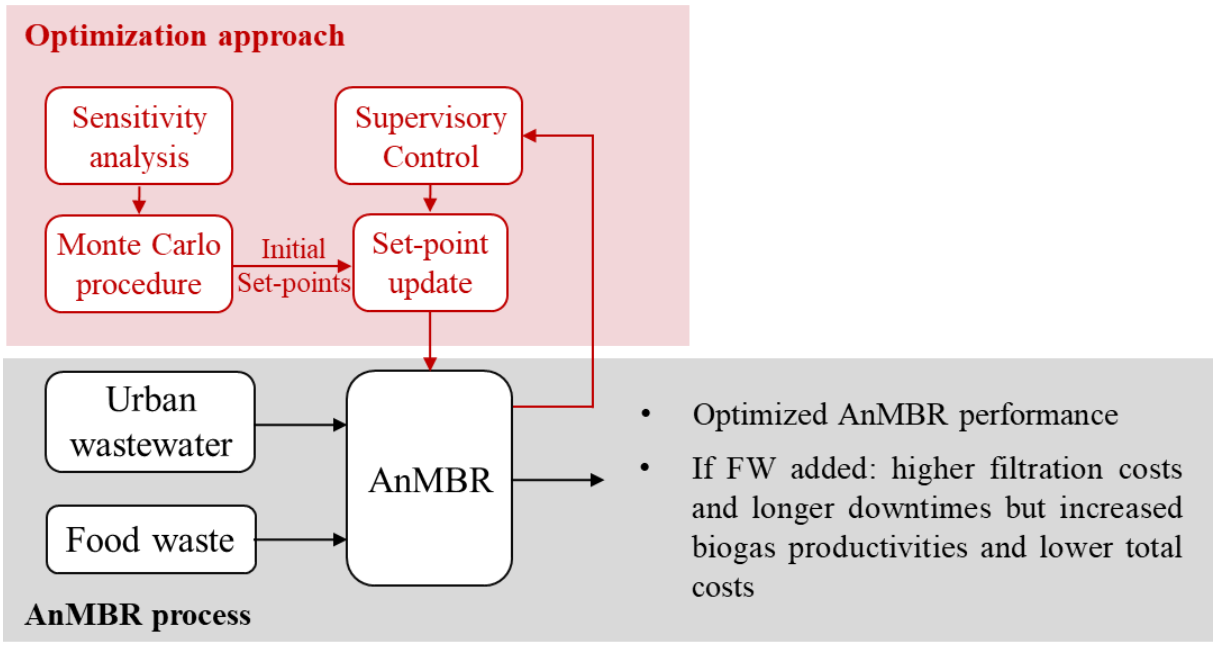

Table 1. Average values of the operational parameters evaluated in this study. The intervals of uncertainty, as well as the initial values for the model-based supervisory controller (Monte Carlo results) are also presented

Parameter	Units	Substrate	Average values	Minimum	Maximum	Monte Carlo results
BRF	$m^3 \cdot h^{-1}$	UWW	12	3	21	13
		UWW +FW	12	3	21	13
SRF	$m^3 \cdot h^{-1}$	UWW	2.1	1.5	2.7	2.0
		UWW +FW	2.1	1.5	2.7	1.8
t_F	s	UWW	400	200	600	600
		UWW +FW	400	200	600	485
t_R	s	UWW	35	10	60	10
		UWW +FW	35	10	60	10
t_{BF}	s	UWW	35	10	60	17
		UWW +FW	35	10	60	31
f_{BF}	-	UWW	11	1	21	10
		UWW +FW	11	1	21	4
J_{BF}	LMH	UWW	15	10	20	16
		UWW +FW	15	10	20	10

Table 2. Sensitivity rankings for r_{opt} with UWW as substrate (r_{opt} = 60) and the mixture of UWW and FW (r_{opt} = 40)

UWW			UWW + FW		
Parameter	**μ^***	**σ**	**Parameter**	**μ^***	**σ**
BRF	1.253	1.856	**BRF**	1.355	2.099
f_{BF}	0.770	2.220	**f_{BF}**	0.579	1.418
t_F	0.724	1.921	**t_{BF}**	0.344	1.059
t_{BF}	0.574	1.210	**t_F**	0.252	0.710
SRF	0.464	1.584	**SRF**	0.163	0.410
t_R	0.057	0.261	**t_R**	0.067	0.138
J_{BF}	0.057	0.268	J_{BF}	0.005	0.018

Table 3. Average energy requirements of the filtration process with the controller operating at 17 $g \cdot l^{-1}$ MLTS entering the membrane tanks

Substrate	**W_{TOTAL} ($kWh \cdot m^{-3}$)**	**W_{BRF} (%)**	**W_{SRF} (%)**	**W_{Stage} (%)**
UWW	0.20	79.7	16.9	14.3
UWW + FW	0.34	88.5	9.6	9.8

Table 4. Average costs of the filtration process with the controller operating at 17 $g \cdot l^{-1}$ MLTS entering the membrane tanks

Substrate	C_{TOTAL} (€ per m^3)	C_W (%)	$C_{REAGENTS}$ (%)	$C_{LIFESPAN}$ (%)
UWW	0.047	59.6	17.0	23.4
UWW + FW	0.067	69.0	13.0	18.0

Figure 1

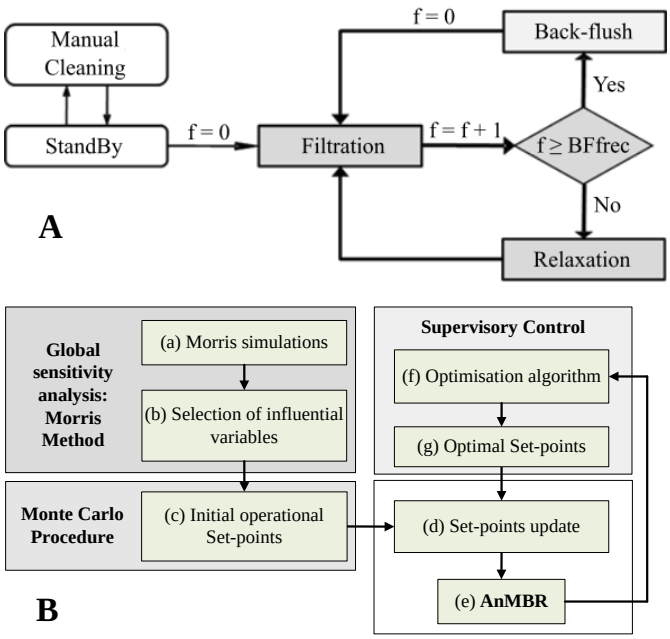

Figure 1. (A) Sequence of the different operational stages in the membrane modules during the alternative operating mode and (B) flow diagram of the proposed optimization methodology

Figure 2

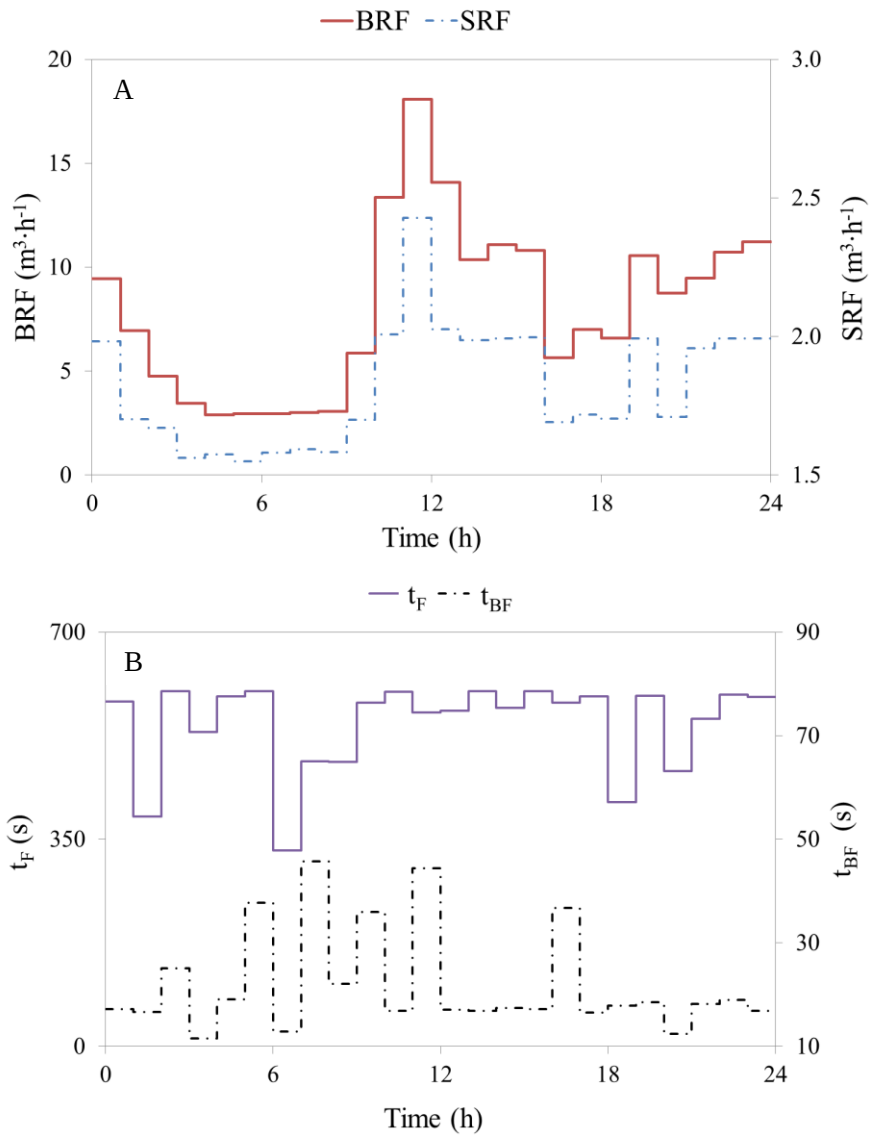

Figure 2. (A) Values of BRF and SRF and (B) t_F and t_{BF} optimized by the supervisory controller. The results were obtained by applying the transmembrane flux shown in Figure S1 with a MLTS concentration entering the tanks of 17 $g \cdot l^{-1}$ and using UWW as substrate

Figure 3

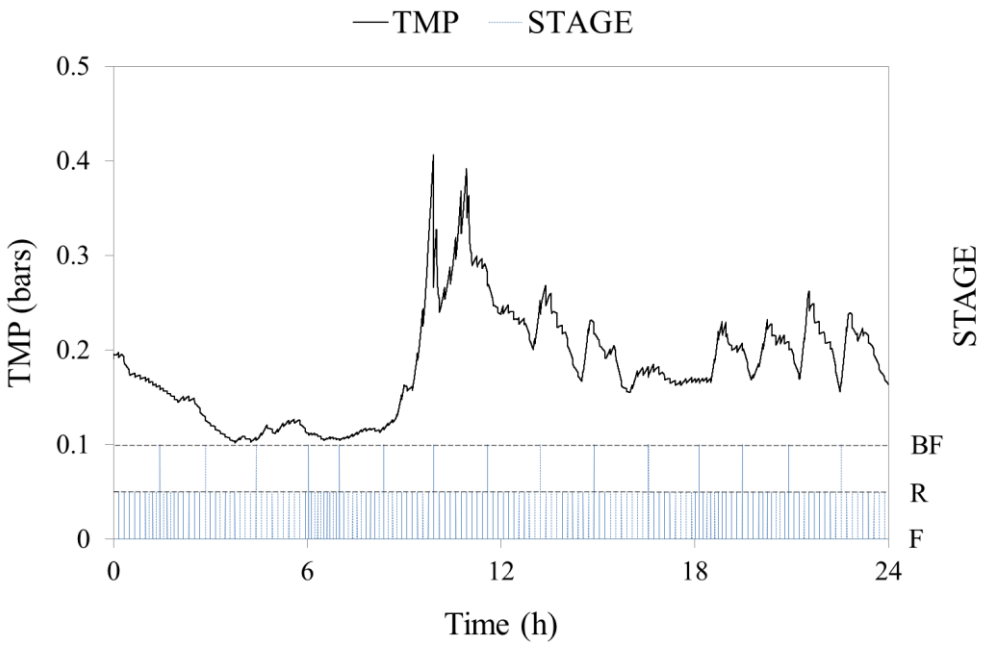

Figure 3. Evolution of the TMPs and different stages simulated. The results were obtained by applying the transmembrane flux shown in Figure S1 with a MLTS concentration entering the tanks of 17 $g \cdot l^{-1}$ and using UWW as substrate

Figure 4

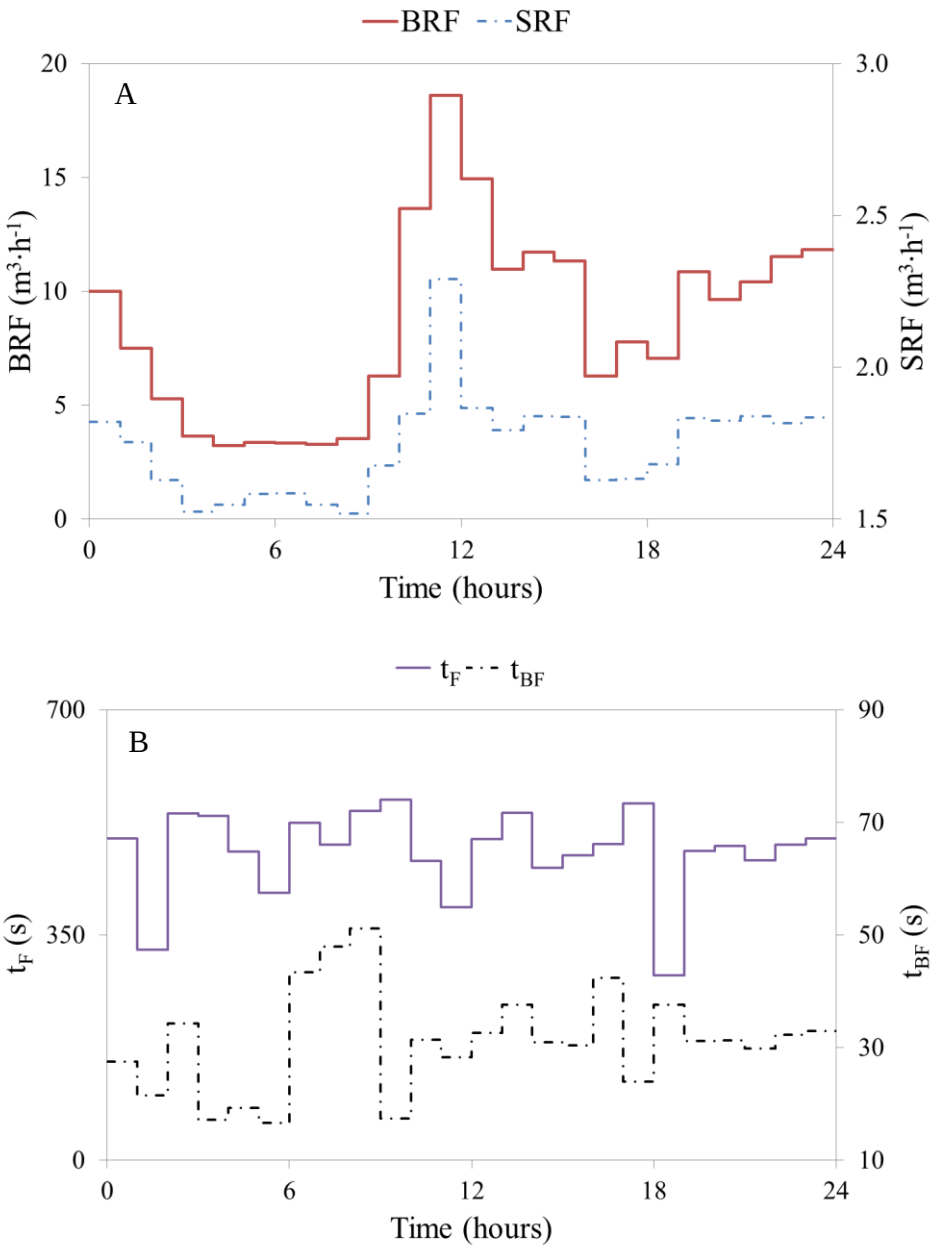

Figure 4. (A) Values of BRF and SRF and (B) t_F and t_{BF} optimized by the supervisory controller. The results were obtained by applying the transmembrane flux shown in Figure S1 with a MLTS concentration entering the tanks of 17 $g \cdot l^{-1}$ and using UWW and FW as substrates

Figure 5

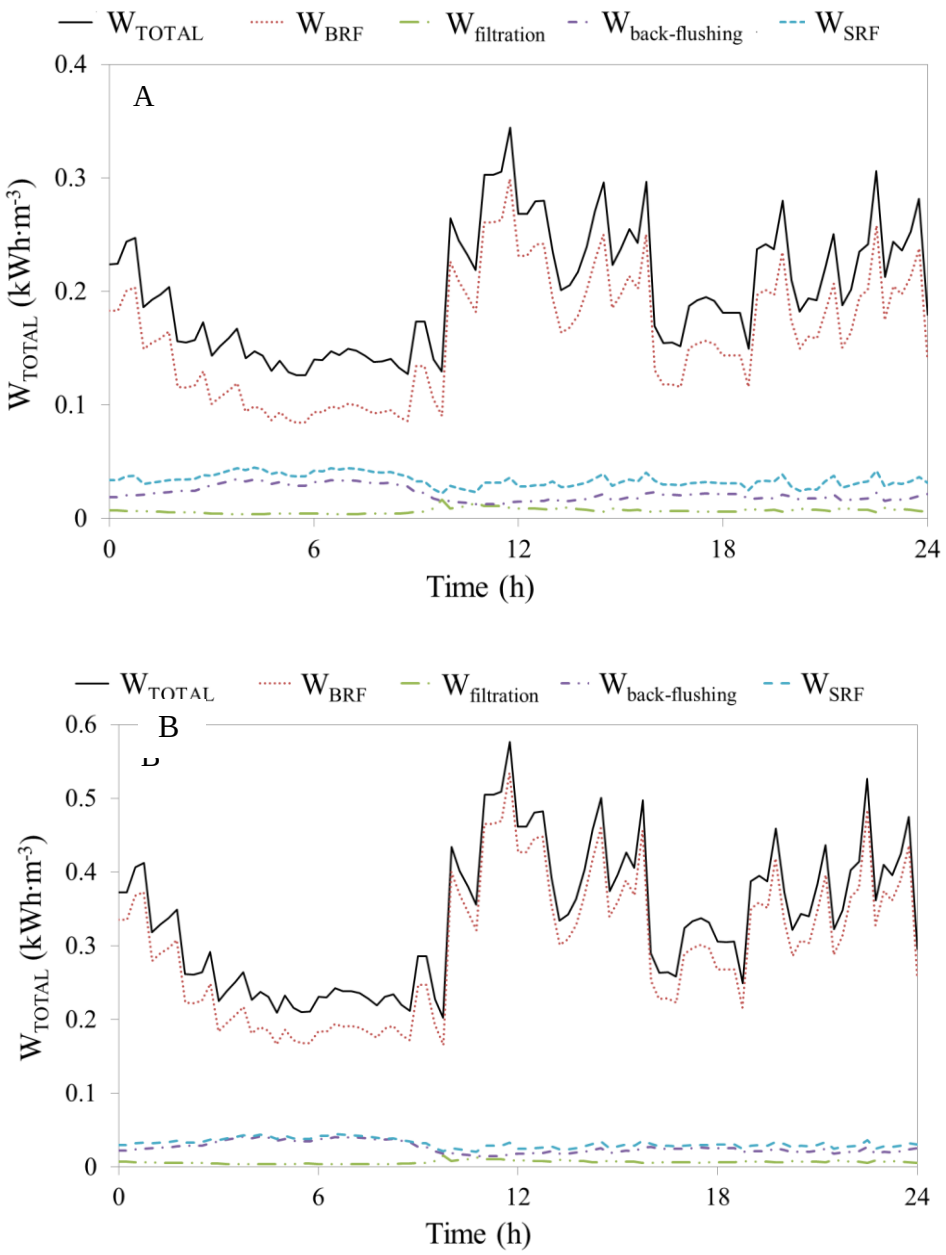

Figure 5. Evolution of the energy requirements of the filtration process with the controller operating at 17 $g \cdot l^{-1}$ MLTS entering the membrane tanks. The results for feeding strategies are shown: (A) UWW and (B) mixture of UWW and FW

Figure 6

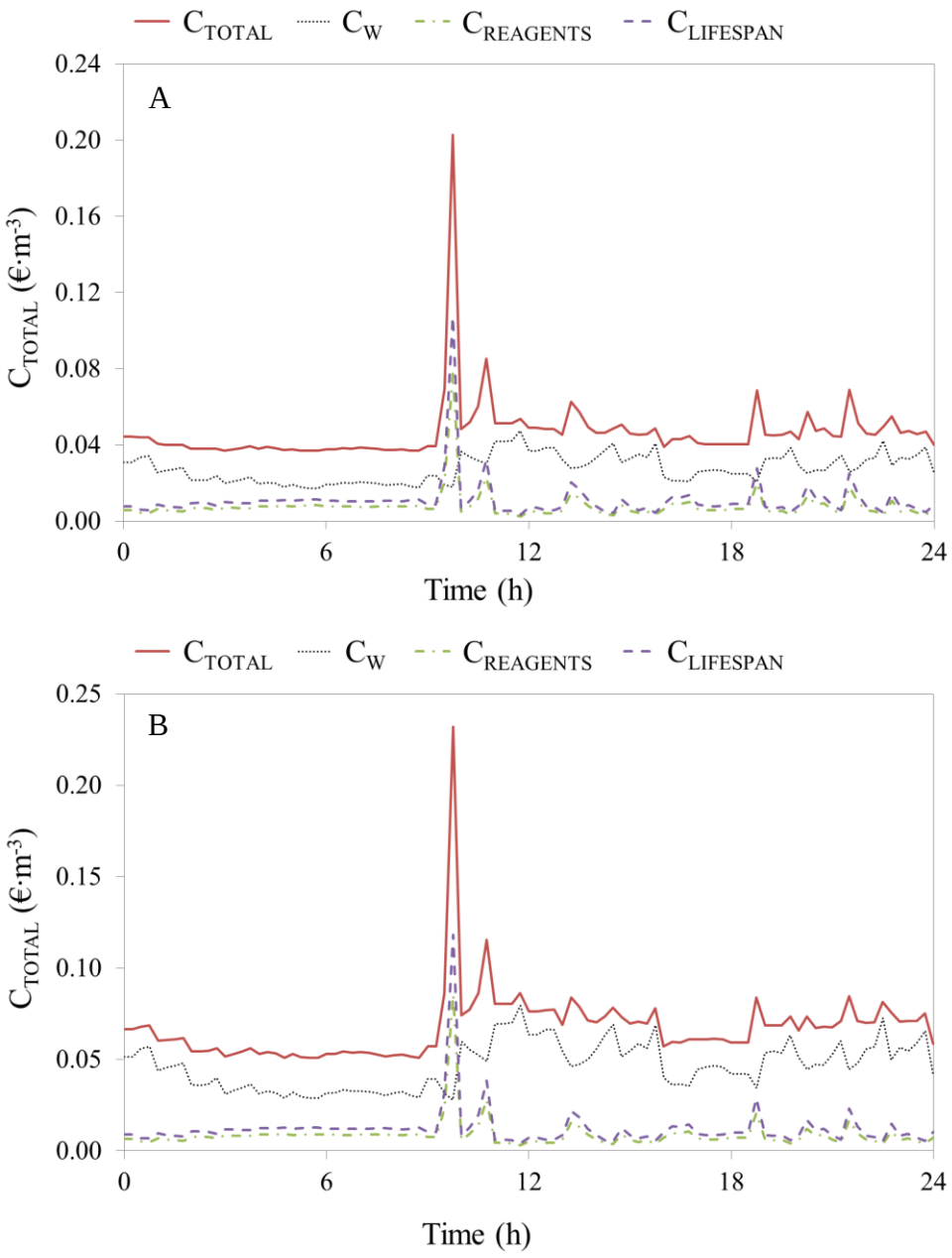

Figure 6. Evolution of the costs of the filtration process with the controller operating at 17 $g \cdot l^{-1}$ MLTS entering the membrane tanks. The results for feeding strategies are shown: (A) UWW and (B) mixture of UWW and FW

E-Component 1

Click here to download E-Component: Figure S1.docx

E-Component 2

Click here to download E-Component: Figure S2.docx

E-Component 3

Click here to download E-Component: Figure S3.docx

E-Component 4

Click here to download E-Component: Figure S4.docx

E-Component 5

Click here to download E-Component: Figure S5.docx